

Correlation between porosity level and elastic modulus in a foamed hiped Ti alloy

GUGLIELMI Pasquale^{1,a*}, CASTELLANO Anna^{1,b}, CUSANNO Angela^{1,c}
and PALUMBO Gianfranco^{1,d}

¹ Politecnico di Bari, Department of Mechanics, Mathematics and Management, Via Orabona 4 - 70125 Bari – Italy

^apasquale.guglielmi@poliba.it, ^banna.castellano@poliba.it, ^cangela.cusanno@poliba.it, ^dgianfranco.palumbo@poliba.it

Keywords: Ti Alloy, Foaming, Hot Isostatic Pressing, Microstructure, Ultrasonic Tests, Young's Modulus

Abstract. Nowadays, in the manufacturing of highly customized prosthetic implants, the need of devices with mechanical properties close to the human bone's ones plays a key role. In the present work, Ti6Al4V-ELI porous structures obtained by a solid-state foaming process were studied from a microstructural and mechanical point of view, being the aim to control the stiffness of the prostheses in order to be as much as possible close to the human bone's one, thus reducing the stress shielding effect. Samples with different levels of porosity (average diameter variable between a few microns and about 50 microns) were investigated by means of contact ultrasonic tests in order to evaluate changes in terms of elastic properties. Metallographic observations combined with contact ultrasonic tests revealed that a good correlation exists between the foamed structure (quantity and average size of the pores) and the stiffness.

Introduction

The human bone can be considered as anisotropic and non-homogeneous material. Moreover, it is capable to vary its shape dynamically according to the stress conditions to which it is subjected [1]. The capability to withstand external stresses is intimately related to both microstructural and macroscopic properties. Many studies evaluated the relationship between architectural factors and large-scale mechanical properties, in terms of fracture risk. Indeed, anisotropy can be correlated both to the modulus of elasticity and strength [2].

In accordance with these considerations, the manufacture of devices for the replacement/repair of damaged bones capable to adapt in the best way to the natural properties of the specific bone through the adoption of metallic materials is still an aspect of primary importance in the biomedical field. Titanium (Ti) and its alloys are extensively used in orthopaedic applications thanks to their (i) good mechanical properties, (ii) biocompatibility [3] and (iii) corrosion resistance [4]. However, large differences in terms of mechanical properties between the prosthesis and the bone to which it is close can cause an alteration of the stress distribution (stress shielding) [5,6]. When considering metallic prostheses, such an aspect plays an important role and cannot be neglected, even for Ti alloys whose elastic modulus is closer to the human bone's one than stainless steels. Thus, the adoption of materials for producing the implants which are characterised by a porous structure can make their stiffness closer to the human bones' one. Ti alloys obtained by means of the Hot Isostatic Pressing (HIP) process of Ti powders can be used for producing such porous materials, since they can develop cellular structures characterised by average porosity up to about 50% by means of a solid state foaming process (i.e. when subjected to constant temperature up to about 1250°C and for appropriate durations) [7]. As result of the foaming process, the mechanical response of the implant is affected. In addition, porosity also affects the surface properties, thus being able to promote the cellular proliferation [4].

Another important aspect in the manufacture of highly customized implants is the need for a perfect fitting between the geometry of the prosthesis and the anatomy of the specific patient; in fact, micro-movements between the two parts can cause the onset of infections [8]. In the light of this non-negligible aspect, increasingly advanced manufacturing technologies, such as additive manufacturing [9], superplastic and incremental forming [10] capable of guaranteeing very complex shapes, are nowadays a functional solution for reducing these risks. In addition, in the specific case of superplastic forming process, which requires the aid of high temperatures, the foaming process could be performed not only after the manufacturing process but also simultaneous with a considerable reduction of both time and costs.

Therefore, the possibility of suitably customising the prosthesis, not only in terms of shape but also of properties (like the stiffness) is a key aspect in the modern medicine. In the present work, according to the one of main goals of the founded national project FabriCARE, the effect of the pressure of the HIP process was evaluated after foaming tests performed at high and constant temperature (1020°C) for 240 minutes. Metallographic aspects, such as the topology of the promoted porosity and the mechanical properties in the elastic field were investigated, respectively by means of light microscopy and ultrasonic tests. Starting from the measurements of the velocity of the bulk (longitudinal and transversal) waves obtained from contact ultrasonic tests, using the linear elastodynamic theory for wave propagation in isotropic material, the elastic moduli of different Ti6Al4V-ELI foam-based specimens were determined. Finally, results from the analyses were correlated and allowed to evaluate the correlation between the average size of the porosities (obtained after the foaming process) and the elastic properties (Young's modulus).

Material and Methods

Material.

The experimental activity was conducted using two different titanium billets produced by Hot Isostatic Pressing (HIP) characterized by process pressure from 80 to 120MPa. For all conditions Ti6Al4V-ELI powders with a diameter from 50 up to 100µm were used. The chemical composition of the investigated material is reported in Table 1.

Table 1. Chemical composition of the investigated Ti6Al4V-ELI alloy.

| Al% | V% | Fe% | C% | N% | H% | O% | Ti |
|------|------|------|------|-------|-------|-------|------|
| 5.88 | 3.87 | 0.14 | 0.22 | 0.006 | 0.002 | 0.112 | Bal. |

Dog-bone specimens (thickness: 3mm) were extracted from the billets using an Electrical Discharge Machine (EDM). The main dimensions of the sample are shown in Fig. 1.

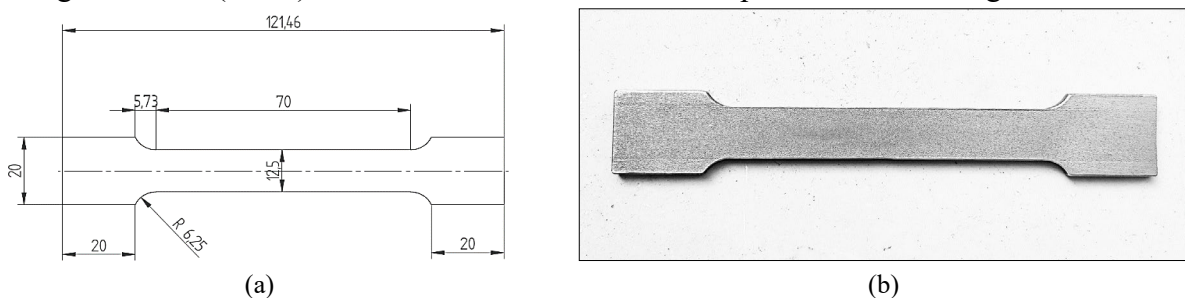


Fig. 1. (a) Main dimensions [mm] of the dog-bone sample extracted by EDM (b) adopted for the foaming tests.

Methodology

Creation of the porous structure.

The porous structure of the specimens to be subjected to ultrasonic tests (Fig. 1) was obtained by solid state foaming, which consists in a heat treatment in the furnace (T=1020°C for 240 minutes [11]). The samples were extracted from billets produced by compacting Ti6Al4V powders (size is in the range 50-100 micron) placed in a sealed can in which the air was replaced by argon gas (pressure: 0.2 MPa) using the HIP process.

In this work, two different levels of the pressure applied during the HIP process were investigated, as summarized in Table 2.

Table 2 Starting conditions of the HIPed samples subjected to foaming.

| | Diameter of titanium powders, μm | Argon pressure, MPa | HIP pressure, MPa |
|-----------------|----------------------------------|---------------------|-------------------|
| D100-A0.2HIP80 | From 50 up to 100 | 0.2 | 80 |
| D100-A0.2HIP120 | From 50 up to 100 | 0.2 | 120 |

Each foaming test was replicated three times; furthermore, the results achieved and subsequently discussed were compared to the “as received” condition (i.e. concerning the specimen extracted from the billet and not subjected to any foaming process).

The level of porosity (percentage area and average diameter of pores) determined by the foaming process was assessed by analysing samples extracted from the central cross sections of the dog-bone specimens: the samples were prepared in order to be observed by an optical microscope (Nikon MA200 equipped with the ImageJ® software for digital image processing).

Young’s modulus evaluation by means of ultrasonic tests

The wave phenomena involved in the ultrasonic tests are usually described by the linearized elastodynamic theory [12], since the ultrasonic waves can be regarded as small perturbations of a reference state of an elastic body. Solutions in the form of progressive plane waves for the equation of motion (Eq. 1) are found

$$\text{Div}(\mathbb{C}[\nabla\mathbf{u}]) = \rho\ddot{\mathbf{u}}, \tag{1}$$

in absence of the body forces, where $\rho = \rho(\mathbf{x})$ is the mass density and $\mathbb{C} = \mathbb{C}(\mathbf{x})$ is the incremental fourth order elasticity tensor referred to the initial state of the body, having the first and the second minor symmetries, and $\mathbf{u} = \mathbf{u}(\mathbf{x})$ has the following form:

$$\mathbf{u}(\mathbf{x},t) = \mathbf{a} \varphi(\mathbf{x} \cdot \mathbf{n} - v t) \tag{2}$$

and represents a progressive elastic plane wave with propagation direction \mathbf{n} , direction of motion \mathbf{a} , propagation velocity v ; φ is a real valued smooth function.

The propagation of plane progressive elastic waves in an elastic body is ruled by the “Fresnel-Hadamard condition” that is the Christoffel equation:

$$[\Gamma(\mathbf{n}) - \rho v^2 \mathbf{I}] \mathbf{a} = \mathbf{o} \tag{3}$$

where $\Gamma(\mathbf{n})$ is the second order Kelvin-Christoffel propagation tensor for the direction \mathbf{n} , related to the elastic tensor \mathbb{C} as follows:

$$\Gamma(\mathbf{n}) = \mathbb{C}^t[\mathbf{n} \otimes \mathbf{n}] \tag{4}$$

where the superscript “t” represents the minor transposition for fourth order tensors.

From Eq. 3, if an elastic wave propagates in a given direction \mathbf{n} , the square of the propagation velocity v is an eigenvalue of the Christoffel tensor $\Gamma(\mathbf{n})$ while the direction of motion \mathbf{a} is the associated eigenvector. The symmetry properties of the elastic tensor \mathbb{C} strongly influence the

features of progressive elastic waves propagating along a certain direction n . Moreover, according to the “Federov-Stippes theorem”, if the elasticity tensor \mathbb{C} is symmetric and strongly elliptic, then at a point x there exists longitudinal (a and n parallel) and transverse (a and n perpendicular) elastic waves. In the case of isotropic material, for each possible direction of propagation n only pure propagation modes like longitudinal waves and transverse waves may propagate. Instead, for anisotropic materials in a generic direction of propagation n , different from a material symmetry axis, elastic waves may propagate in a not pure propagation modes (as “quasi-longitudinal” waves or as “quasi-transverse” waves).

This theoretical framework suggests a non-destructive ultrasonic experimental counterpart: indeed, the results of ultrasonic tests can be employed for facing two major problems in the mechanics of elastic materials: (i) the *classification problem*, that is the determination of the symmetry class and the identification of the material symmetry axes; (ii) the *representation problem*, that is, once known the symmetry class, the determination of the components of the elastic tensor \mathbb{C} characterizing the elastic response of the material.

For the study of acoustic and mechanical behaviour of *porous* Ti6Al4V-ELI specimens the theoretical model of the isotropic material was adopted. So, by the inversion of the Christoffel equation (Eq. 3), the well-known expression in Eq. 5 have been obtained.

$$E = \rho v_T^2 \frac{3v_L^2 - 4v_T^2}{v_L^2 - v_T^2}, \quad G = \rho v_T^2, \quad \nu = \frac{\left(\frac{v_L}{v_T}\right)^2 - 2}{2 \left[\left(\frac{v_L}{v_T}\right)^2 - 1\right]} \quad (5)$$

between the elastic properties (the Young’s modulus E , the shear modulus G and the Poisson’s ratio ν), the velocity of longitudinal waves v_L and of transversal waves v_T and the density ρ .

The ultrasonic tests were performed at the Laboratorio Ufficiale Prove Materiali “M. Salvati” (Polytechnic University of Bari). In particular, ultrasonic tests were carried out by contact through the pulse-eco (or back reflection) technique, i.e. a single transducer is employed that emits and receives the ultrasonic signal. For the sake of brevity, only the results of the contact ultrasonic tests are shown. The ultrasonic immersion tests carried out using an innovative goniometric device [13] gave results similar to those of the ultrasonic contact tests.

The experimental setup of the contact ultrasonic tests (Fig. 2a) consists in: (1) an ultrasonic pulser/receiver Panametrics 5072PR for generating and receiving the ultrasonic waves; (2) a digital oscilloscope KEYSIGHT DSOS254A (2.5 GHz, 4 channels) for monitoring the ultrasonic signals; (3) an ultrasonic 5 MHz longitudinal wave contact transducer; (4) an ultrasonic 2.25 MHz transversal waves contact transducer; (5) a PC controlling the test.

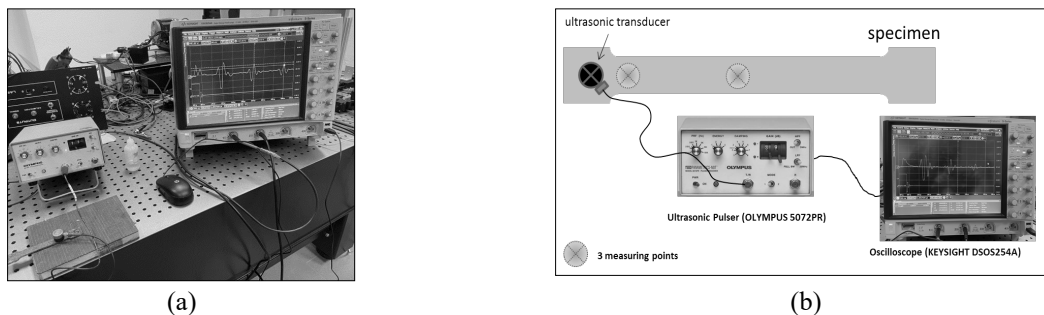


Fig. 2. Ultrasonic contact tests setup: (a) main components and (b) a schematic drawing showing the TOF measuring points.

In particular, for each of the five samples, three time-of-flight (TOF) measurements of both longitudinal and transverse waves were performed. Such TOF measurements were performed in three different areas of the sample, as shown in Fig. 2b.

It is worth noticing that the TOF measurements were carried out through an averaging process of the acquired and normalized ultrasonic signals for each area of the tested specimens performed by the ad hoc developed Virtual Instrument (VI) created using the software LabView. So, starting from the TOF of the ultrasonic waves, known the thickness s of each of the three measurement zones in the sample, that is the spatial path of the wave in the material, the ultrasonic velocities v of the longitudinal waves and of the transversal waves were determined, respectively, by using:

$$v = \frac{2s}{TOF} \tag{6}$$

being $2s$ the wave path (the double of the thickness of the material).

Finally, known the density of each Ti6Al4V-ELI foam-based specimens, by implementing in the Eq. 5 the average values of the ultrasonic velocities, the elastic moduli were determined.

Results and Discussion

Experimental foaming tests Fig. 3 shows the micrographs of different sections of the foamed samples at a constant temperature of 1020°C for 240 minutes. It is possible to evaluate the effect of the HIP process conditions (in accordance with the values reported in Table 2).

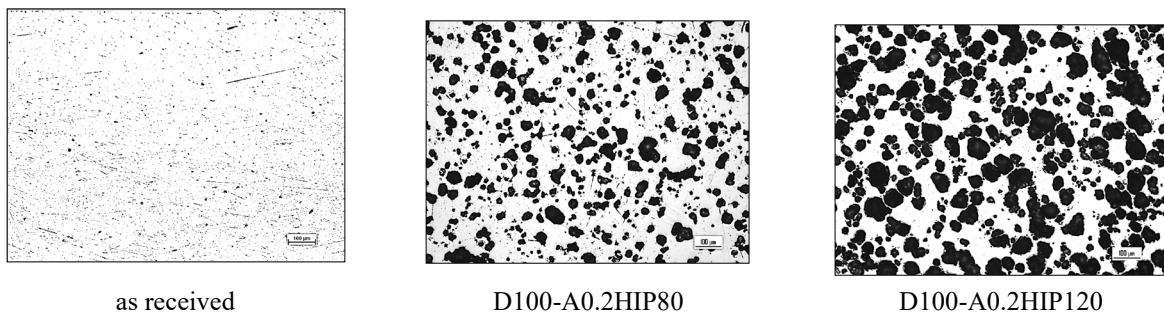


Fig. 3. Effect of the HIP conditions on the solid-state foaming after 240 minutes at 1020°C.

In the same Fig. 3 it is possible to appreciate the large difference between the foamed conditions and the as received one. The reported micrographs suggest that by increasing the HIP process pressure the porosity of the structure can be largely affected. It is thus reasonable to expect significant variations in terms of elastic properties of the material.

The images from the metallographic observations were also analysed quantitatively: in particular, the level of porosity was evaluated in terms of both average area (%) and average size (porosity diameter). Results have been reported in Fig. 4.

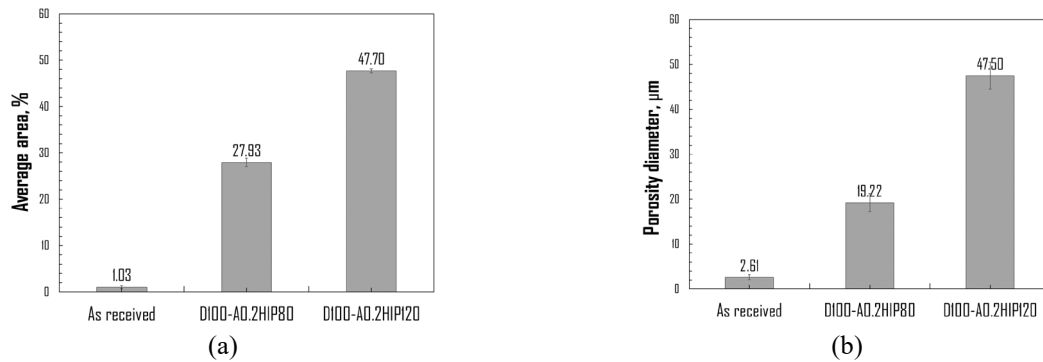


Fig. 4. Effect of the HIP conditions in terms of Average area (a) and Average size (b) of the porosity.

It is interesting to note that after the foaming process the percentage area of voids varies from a minimum of about 1% (for the as received condition) to a maximum of 47.7% (D100-A0.2HIP120). At the same time, the average size of the pores varies from 2.61 to 47.50μm.

According to the graphs in Fig. 4, an increase in the HIP pressure from 80 to 120 MPa allowed to obtain an increase of the porosity equal to about 42%, while an increase in the average size of about 60%.

Experimental ultrasonic tests.

This section presents some results from ultrasonic tests aimed at determining the elastic properties of the investigated material after the foaming process. In particular, the attention was focused on the Young's modulus, whose values were compared with the elastic modulus obtained same alloy deriving from a conventional process and tested in "as received" condition.

The graphs in Fig. 5 show the results in terms of ultrasonic velocities and level of porosity. In both graphs, it is possible to observe a variation in the acoustic behavior of the specimens and a variation of the level of porosity, as well. In particular, it is worth noticing that as the porosity increases, the values of the velocities of both the longitudinal and the transversal waves decrease.

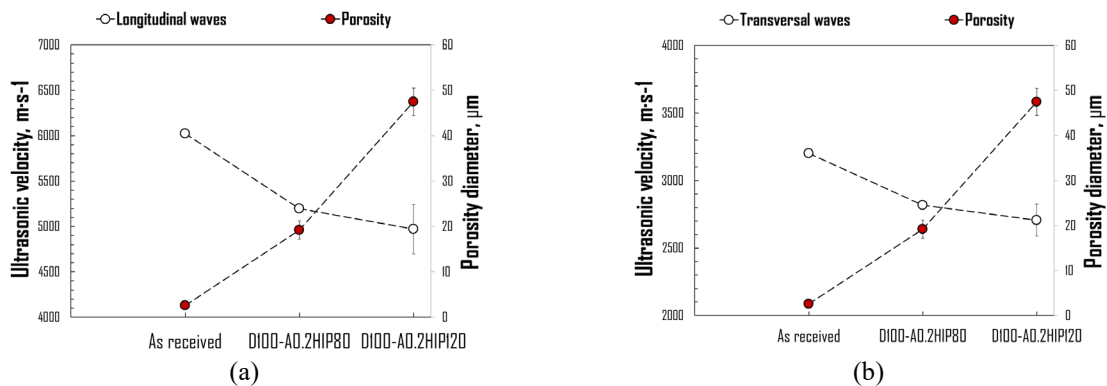


Fig. 5. Ultrasonic velocities of the longitudinal (a) and transversal (b) waves measured according to the different levels of porosity.

On the contrary, in the graphs in Fig. 6 the values of the elastic moduli determined using Eq. 5 have been plotted together with the levels of porosity.

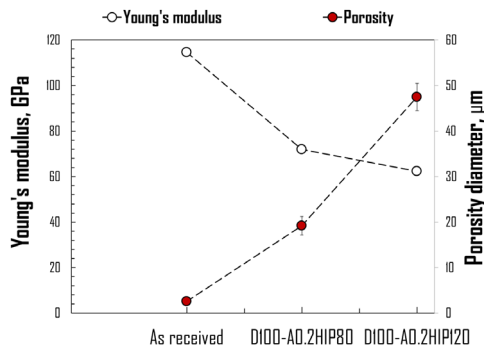


Fig. 6. Young's modulus for each Ti6Al4V-ELI foam-based specimen as a function of the different levels of porosity.

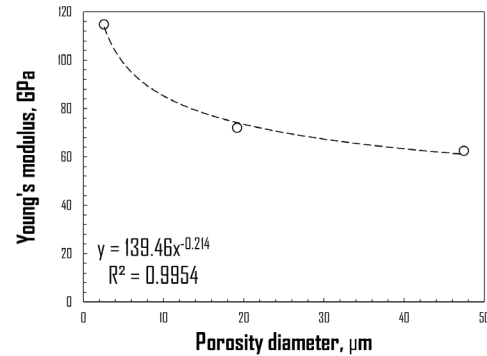


Fig. 7. Correlation between the level of porosity (Average diameter) and the Young's modulus evaluated using the ultrasound technique.

Also in terms of mechanical properties, a large decrease of the elastic moduli can be observed when the porosity increases: the Young's modulus was reduced from 114 GPa (the alloy in the “as received” condition) to about 62 GPa, when the maximum value of the HIP pressure was used. If compared to the “as received” condition, the increase in the HIP pressure allows to produce a porous structure, after the foaming process, able to drastically (about 45 %) reduce the elastic properties.

In addition, it is worthy of notice that a strong correlation between the porosity after the foaming process and the elastic properties could be determined (Fig. 7): using a power law data could be correlated in a robust way (R-squared equal to 0.995), thus demonstrating the possibility to efficiently design the elastic response of the material through the definition of the porosity level which, in turn, is controlled by the foaming process.

Summary

In the present work different porosity levels after the foaming process (T=1020°C for 240 minutes) were obtained in specimens extracted from a billet produced by means of the Hot Isostatic Pressing (HIP) process of Ti powders.

Results coming from metallographic analyses allowed to evaluate an improved foaming capability (average porosity equal to about 60%) as the HIP pressure was increased from 80 to 120MPa.

In addition, ultrasonic contact tests allowed to evaluate the mechanical properties of the porous material obtained by the foaming process, which revealed to largely affect the stiffness (Young's modulus decreases when the porosity increases). The Young's modulus could be thus correlated to the level of porosity through a power function, thus paving the way to the customization of the prosthesis not anymore only in terms of shape according to the specific anatomy of the patient but also in terms of mechanical properties.

References

- [1] E. F. Morgan, G.U. Unnikrisnan, A.I. Hussein, Bone Mechanical Properties in Healthy and Diseased States, *Annu. Rev. Biomed. Eng.* 20 (2018) 119-143. <https://doi.org/10.1146/annurev-bioeng-062117-121139>.
- [2] D. Wu, P. Isaksson, S.J. Ferguson, C. Persson, Young's modulus of trabecular bone at the tissue level: A review, *Acta Biomater.* 78 (2018) 1-12. <https://doi.org/10.1016/j.actbio.2018.08.001>

- [3] Y. Guo, F. Liu, X. Bian, K. Lu, P. Huang, X. Ye, C. Tang, X. Li, H. Wang, K. Tang, Effect of Pore Size of Porous-Structured Titanium Implants on Tendon Ingrowth, *Appl. Bionics Biomech.* 2022 (2022). <https://doi.org/10.1155/2022/2801229>
- [4] M. Chimumtengwende-Gordon, R. Dowling, C. Pendegrass, G. Blunn, Determining the porous structure for optimal soft-Tissue ingrowth: An in vivo histological study, *PLoS One* 13 (2018) 1-17. <https://doi.org/10.1371/journal.pone.0206228>
- [5] M. Niinomi, M. Nakai, J. Hieda, Development of new metallic alloys for biomedical applications, *Acta Biomater.* 8 (2012) 3888-3903. <https://doi.org/10.1016/j.actbio.2012.06.037>
- [6] C. Piao, D. Wu, M. Luo, H. Ma, Stress shielding effects of two prosthetic groups after total hip joint simulation replacement, *J. Orthop. Surg. Res.* 9 (2014) 1-8. <https://doi.org/10.1186/s13018-014-0071-x>
- [7] S. Oppenheimer, D.C. Dunand, Solid-state foaming of Ti-6Al-4V by creep or superplastic expansion of argon-filled pores, *Acta Mater.* 58 (2010) 4387-4397. <https://doi.org/10.1016/j.actamat.2010.04.034>
- [8] G. Palumbo, G. Ambrogio, A. Crovace, A. Piccininni, A. Cusanno, P. Guglielmi, L. De Napoli, G. Serratore, A Structured Approach for the Design and Manufacturing of Titanium Cranial Prostheses via Sheet Metal Forming, *Metals* 12 (2022) 293. <https://doi.org/10.3390/met12020293>
- [9] J. Barrios-Muriel, F. Romero-Sánchez, F.J. Alonso-Sánchez, D.R. Salgado, Advances in orthotic and prosthetic manufacturing: A technology review, *Materials* 13 (2020) 295. <https://doi.org/10.3390/ma13020295>
- [10] G. Ambrogio, G. Palumbo, E. Sgambitterra, P. Guglielmi, A. Piccininni, L. De Napoli, T. Villa, G. Fragomeni, Experimental investigation of the mechanical performances of titanium cranial prostheses manufactured by super plastic forming and single-point incremental forming, *Int. J. Adv. Manuf. Technol.* 98 (2018) 1489-1503. <https://doi.org/10.1007/s00170-018-2338-6>
- [11] P. Guglielmi, A. Piccininni, A. Cusanno, A.A. Kaya, G. Palumbo, Mechanical and microstructural evaluation of solid-state foamed Ti6Al4V-ELI alloy, *Procedia CIRP* 110 (2022)105-110. <https://doi.org/10.1016/j.procir.2022.06.021>
- [12] M.E. Gurtin, The linear theory of elasticity, in: *Linear theories of elasticity and thermoelasticity*, Springer, 1973.
- [13] A. Castellano, P. Foti, A. Fraddosio, S. Marzano, M.D. Piccioni, Mechanical characterization of CFRP composites by ultrasonic immersion tests: Experimental and numerical approaches, *Compos. Part B Eng.* 66 (2014) 299-310. <https://doi.org/10.1016/j.compositesb.2014.04.024>